Electromagnetic absorption characteristics of manganese-zinc ferrite and multiwalled carbon nanotube-filled composites based on NBR

ELECTROMAGNETIC ABSORPTION CHARACTERISTICS OF MANGANESE-ZINC FERRITE AND MULTIWALLED CARBON NANOTUBE-FILLED COMPOSITES BASED ON NBR

Ján Kruželák,[1,*] Andrea Kvasničáková,[1] Klaudia Hložeková,[1] Michaela Džuganová,[1] Jana Gregorová,[1] Jarmila Vilčáková,[2] Marek Gořalík,[3] Ján Hronkovič,[4] Jozef Preťo,[4] Ivan Hudec[1]

[1]*Department of Plastics, Rubber and Fibres, Faculty of Chemical and Food Technology, Slovak University of Technology in Bratislava, Radlinskeho 9, 812 37 Bratislava, Slovakia*

[2]*Centre of Polymer Systems, University Institute, Tomas Bata University in Zlín, Třída Tomáše Bati 5678, 760 01 Zlín, Czech Republic*

[3]*Polymer Centre, Faculty of Technology, Tomas Bata University in Zlín, Vavrečkova 275,760 01 Zlín, Czech Republic*

[4]*VIPO a.s., Gen. Svobodu 1069/4,958 01, Partizánske*

[*]*Corresponding author. Email: jan.kruzelak@stuba.sk*

Abstract

Composites based on acrylonitrile-butadiene rubber, carbon nanotubes, and manganese-zinc ferrite were fabricated and tested for electromagnetic interference (EMI) absorption shielding. First, carbon nanotubes and ferrite were solely used for the preparation of rubber composites. Then, carbon nanotubes were combined with magnetic filler and incorporated into the rubber matrix. The results revealed that carbon nanotubes act as reinforcing filler and significantly enhance the physical-mechanical properties of composites. The presence of carbon nanotubes in the rubber matrix also results in an outstanding increase in electrical conductivity and permittivity of composite materials, as a consequence of which the EMI absorption shielding was poor in the tested frequency range of 1 MHz to 3 GHz. On the other hand, ferrite-filled composites are able to efficiently absorb electromagnetic radiation emitted from various electronic and radiation sources. However, the tensile strength of the composites showed a decreasing trend with increasing content of ferrite. The combination of carbon nanotubes with manganese-zinc ferrite resulted in an improvement in the physical-mechanical properties of hybrid composites. As the permittivity of hybrid composites was still much higher in comparison with those filled only with ferrite, only the composite filled with 5 phr of carbon nanotubes and 100 phr of ferrite showed a slight EMI absorption shielding ability over the tested frequency range. [doi:10.5254/rct.22.77986]

INTRODUCTION

The rapid progress in industrialization and informatization of today‘s modern society has led to the generation of a high amount of environmental pollution. This pollution is mainly associated with

electromagnetic radiation accumulated in the surrounding environment, and it is often termed electromagnetic smog or electromagnetic interference (EMI). EMI can be explained as the undesired disturbances in electronic appliances, which is caused by the interference of multiple electromagnetic signals transmitting from neighboring devices. It has been reported that EMI interrupts the functionality of electronic devices and may also have harmful effects on the living environment of human beings.[1,2] To overcome the problem, materials with EMI shielding effectiveness are highly required. Traditionally, metal-based EMI shielding materials have been widely used because of their excellent electrical conductivity. However, high weight, poor flexibility, heavy manipulation, and high prices limit the utilization of those materials. Another point arising from their high conductivity is a high proportion of reflection shielding. Shielding by reflection seems to be undesirable, because reflected electromagnetic waves can easily interfere with initial electromagnetic radiation, which results in a higher accumulation of EMI in the surrounding environment. Polymer composites with excellent electromagnetic characteristics can be used as an alternative to conventional metal-based EMI shields because of their flexibility, low specific weight, corrosion resistance, good processability, tunable properties, and low cost.[3] The electromagnetic characteristics of the polymer matrices can be imparted by the incorporation of suitable fillers. The incorporation of fillers into polymer matrices provides space not only for tuning structural and mechanical properties of the corresponding composites but also for enabling the adjustment of permeability, permittivity, electrical conductivity, and thickness to achieve desirable EMI performance.

Ferrites are ceramic materials composed of various oxides with iron oxide as their main constituent. They exhibit high resistivity, high permeability, a wide range of operating frequencies, good chemical stability, low losses, temperature stability, and low price.[4] They have been integrated in electrical components, choke coils, memory chips, magnetic and magnetic-optical recordings, telecommunication, automobiles, and so forth.[5,6] Possessing low eddy current and dielectric losses, they have also been widely used in high-frequency applications, as RF transformers or inductors. The properties of ferrites can be easily modified by preparation conditions or the nature of substituents. The very good ability of ferrites to attenuate electromagnetic waves enables their use as microwave absorbers.[7-9]

Carbon nanotubes are allotropes of sp^2-bonded carbon atoms that have tubular nanostructures. These cylindrical carbon molecules have unusual properties that are valuable for nanotechnology, electronics, optics, actuators, sensors, capacitors, and other fields of materials science, biomedical science, and technology.[10] Because of their the small diameter, high aspect ratio, low specific weight, exceptional electrical and thermal conductivity, and high mechanical strength, carbon nanotubes are more advantageous materials over traditional carbon-based fillers, and desired EMI shielding performance can be easily achieved at relatively low contents in polymer matrices.[11-13]

The increasing demands associated with eliminating or reducing EMI have focused the research interest on the development on materials with electromagnetic absorption performance, which can efficiently absorb electromagnetic radiation and dissipate it into other forms of energy, for example, heat.

Many studies have been aimed at the application of magnetic fillers or carbon nanotubes into polymer matrices to prepare composites with the ability to shield electromagnetic radiation emitted from various electronic and radiation sources.[14-19] The studies revealed that polymer composites filled with those fillers exhibit EMI shielding performance. Most studies have been focused on shielding effectiveness at high frequencies, mainly over the X-band frequency range (8.2-12.4 GHz) or even higher frequencies. Commonly used electronic devices (mobile phones, TV sets, radios, laptops, etc.) emit electromagnetic radiation at much lower frequencies, usually from 0.1 GHz to 3 GHz.[20,21] Thus,

the investigation of electromagnetic shielding effectiveness of composites at low frequencies is also very important. In the current work, manganese-zinc ferrite or carbon nanotubes were solely incorporated into arubber matrix based on NBR. Subsequently, both fillers were applied to rubber compounds at certain ratios, and the absorption shielding ability of the composite materials was investigated at low frequencies.

EXPERIMENTAL

MATERIALS

Acrylonitrile-butadiene rubber NBR (SKN 3345, acrylonitrile content 31-35%) supplied from Sibur International (Moscow, Russia) was used as rubber matrix. The rubber batch based on NBR and multiwalled carbon nanotubes (MWCNTs; NC7000, length 1.5 μm, diameter 9.5 nm, content of carbon 90%, specific surface area 250-300 m^2/g) was provided from Nanocyl SA (Sambreville, Belgium). The amount of MWCNT in the rubber batch was 25 parts per hundred parts of rubber (phr).

Table I Characteristics of Manganese-Zinc Ferrite

Characteristic	Value
Particle size, μm	0.1–30
Specific surface area, m^2/g	10.99
Total porosity, %	59.72
Density, g/cm^3	4.87
Electrical resistivity, Ω.m	3

Manganese-zinc ferrite MnZn provided by Epcos s.r.o (Moravičany, Czech Republic) was used as a magnetic soft ferrite filler. The structural characteristics of manganese-zinc ferrite are summarized in **Table I**. A standard sulfur-based curing system consisting of stearic acid and zinc oxide (Slovlak, Košeca, Slovakia) as activators, accelerator N-cyclohexyl-2-benzothia-zole sulfenamide CBS (Duslo, Šaľa, Slovakia), and sulfur (Siarkopol, Tarnobrzeg, Poland) was used for cross-linking of composite materials.

METHODS

Preparation and Curing of Rubber Compounds. — Three types of composites were fabricated and tested for electromagnetic shielding efficiency. $MWCNTs$ in the amount ranging from 2.5 to 25 phr were dosed to the first type of composites. In the second type of composites, manganese-zinc ferrite in a concentration scale ranging from 100 to 500 phr was used. In the third type of rubber compounds, the content of the carbon nanotubes was kept constant at 5 phr, and the amount of manganese-zinc ferrite was changed from 100 to 500 phr. The composition of the rubber compounds is given in **Table II**.

The compounding of additives was performed using Brabender laboratory kneading equipment (Brabender GmbH & Co. KG, Duisburg, Germany). The speed of the rotor was set to 50 rpm, and the kneading chamber was heated to 90 °C. For the preparation of rubber compounds with carbon nanotubes, NBR was first put into the chamber to reduce the amount of $MWCNT$ in the rubber batch to the required concentration. The $NBR/MWCNT$ batch was subsequently added. The compounding of ingredients took 2.5 min. Stearic acid and ZnO were then added with subsequent mixing for 6.5 min. CBS and sulfur were introduced in the second step (4 min, 90 °C, 50 rpm). Finally, the two-roll calender was introduced to form the prepared compounds into thin rubber sheets.

In the case of rubber compounds filled with ferrite, NBR was first plasticated for 2.5 min, followed by the addition of activators, and after 2 min, the filler was applied. The total time of the first-step mixing was 9 min at 90 °C and 50 rpm. In the second step (4 min, 90 °C, 50 rpm), the accelerator CBS and sulfur were introduced. Finally, the rubber compounds were homogenized in a two-roll calender.

Table II Composition of Composites Filled with Carbon Nanotubes (Formulation 1), Composites Filled with Ferrite (Formulation 2), and Composites Filled with Combination of Ferrite and Carbon Nanotubes (Formulation 3)

	NBR	ZnO	Stearic acid	CBS	Sulfur	MWCNT	Ferrite
Formulation 1	100	3	2	1.5	1.5	2.5–25	
Formulation 2	100	3	2	1.5	1.5		100–500
Formulation 3	100	3	2	1.5	1.5	5	100–500

The preparation procedure of the rubber compounds filled with carbon nanotubes and magnetic filler proceeded in the same way as in the previous case, but the $NBR/MWCNT$ batch was first compounded with pure NBR to reduce the amount of carbon nanotubes to 5 phr. Then, the compounding procedure followed the same conditions.

The curing process of the rubber compounds was performed at 160 °C for the optimum curing time under a pressure of 15 MPa by using a hydraulic press (Fontijne, Vlaardingen, the Netherlands). Finally, thin sheets (width 15 × 15 cm, thickness 2 mm) of the cured rubber compounds were obtained.

$Investigation\ of\ Physical-Mechanical\ Characteristics.$ — The tensile properties of the composites were evaluated by using the Zwick Roell/Z 2.5 appliance (Zwick Roell Group, Ulm, Germany). The cross-head speed of the measuring device was set to 500 mm/min, and the tests were carried out in compliance with the valid technical standards. Dumbbell-shaped test specimens (thickness 2 mm, length 80 mm, width 6.4 mm) were used for measurements.

$Investigation\ of\ Shielding\ Characteristics.$ — The frequency dependences of complex permeability and complex permittivity of the prepared composite materials were measured in the range of 1 MHz to 3 GHz by means of a combined impedance/transmission line method using a vector network analyzer (Keysight E5063A, Keysight Technologies, Santa Rosa, CA, USA). The DC electrical conductivity of the composites was determined using the standard two-probe method. Based on the frequency responses of the material parameters, the monolayer electromagnetic wave absorption characteristics (return loss RL, matching thickness d_m, matching frequency f_m, bandwidth Δf for RL at —10 dB and RL at —20 dB, and the minimum of return loss RL_{min}) were computed from return loss RL. This was defined as follows:

$$RL = 20\log\left|\frac{Z_{in} - Z_0}{Z_{in} + Z_0}\right| \quad (1)$$

where

$$Z_{in} = \sqrt{\frac{\mu}{\varepsilon}}\tan\left|i\frac{\omega d}{c}(\mu.\varepsilon)\right| \quad (2)$$

In this equation, Z_{in} is the normalized value of the input complex impedance of the absorber, Z_0 is the wave impedance of free space, ω is the angular frequency, c is the velocity of light in free space, d is the thickness of the monolayer absorber (backed by a metal sheet), and ε and μ are complex permittivity and permeability. The composite absorbs the maximum of the energy if $Z_{in} = 1$, which is reached at a matching thickness $d = d_m$, matching frequency $f = f_m$, and minimum return loss $RL = RL_{min}$.

$Microscopic\ Analysis.$ — The surface morphology and microstructure of the composites were observed using the scanning electron microscope (SEM) JEOL JSM-7500F (Jeol Ltd., Tokyo, Japan). The samples were first cooled in liquid nitrogen under a glass transition temperature and then fractured into small fragments with a surface area of 3 × 2 mm. The fractured surface was covered with a thin layer of gold and put into the microscope. The source of the electrons was a cold-cathode UHV field emission gun, with an accelerate voltage ranging from 0.1 kV to 30 kV and resolution of 1.0 nm at 15kV and 1.4 nm at 1 kV. The SEM images were captured by a CCD camera (EDS, INCA X-ACT, Oxford Instruments, Abingdon, UK).

$Rheological\ Measurement.$ — The rheological properties of the rubber compounds were investigated using RPA 2000. The samples were analyzed using a strain sweep test at a shear rate ranging from 0.01 to 50 s^{-1}, constant frequency of 0.2 Hz, and temperature of 90 °C.

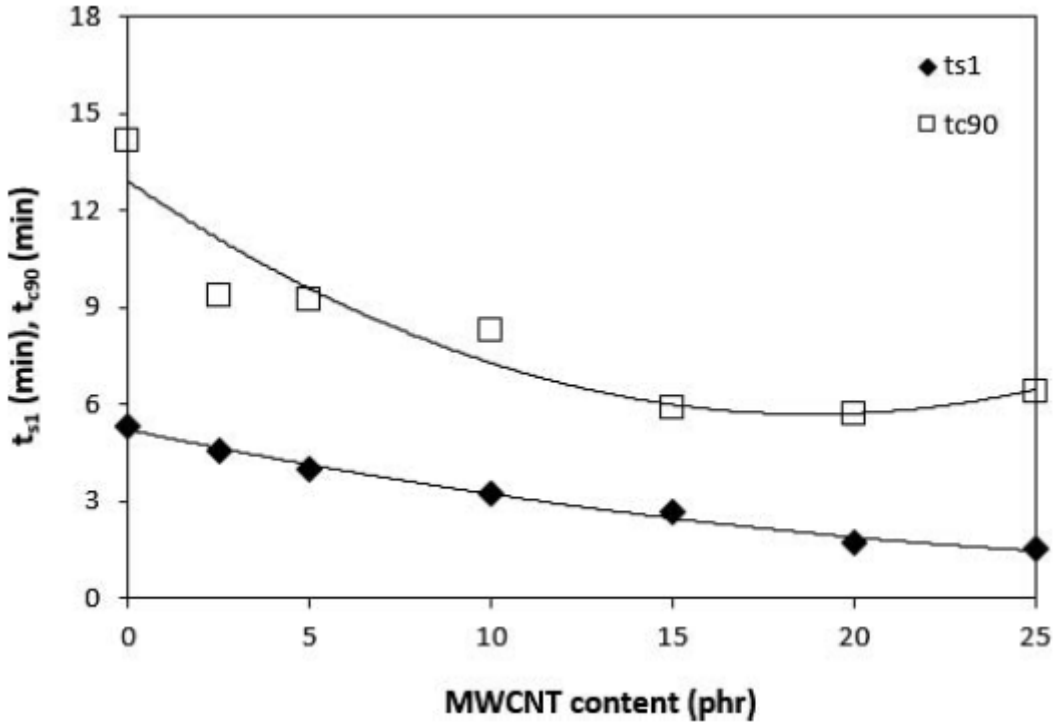

FIG. 1. — Influence of MWCNT content on scorch time t_{s1} and optimum cure time t_{c90} of rubber compounds.

RESULTS AND DISCUSSION

INFLUENCE OF CARBON NANOTUBES ON PHYSICAL-MECHANICAL AND SHIELDING PROPERTIES OF COMPOSITES

The first part of the study was aimed at the preparation of composites filled with carbon nanotubes. The amount of the filler ranged from 2.5 to 25 phr. The composites were cured at 160 °C with the use of a standard sulfur-based curing system. From **Figure 1**, it is apparent that the scorch time ts1 showed a decreasing trend with increasing content of carbon nanotubes. By increasing the content of the $MWCNT$ from 0 up to the maximum content, the scorch time decreased from 5.5 to 1.5 min. The application of the $MWCNT$ also resulted in a decrease in the optimum cure time tc90 up to roughly 15 phr of the filler, and then it settled almost at constant values. The decrease in both curing characteristics with an increase in filler content points out the acceleration of the curing process, which can be attributed to the increase in the thermal conductivity of the rubber compounds due to the presence of carbon filler. The higher the amount of carbon nanotubes, the higher the thermal flow through the composites and the higher the heating up to the curing temperature.

The absorption shielding effectiveness of composites was investigated in the frequency range from 1 MHz to 3 GHz. Because generally used electronic devices emit electromagnetic radiation in the frequency range of 0.1-3 GHz, the composites used as efficient EMI shields should exhibit absorption maxima over this frequency range.

The frequency dependences of real ε' and imaginary ε'' parts of the complex (relative) permittivity $\varepsilon = \varepsilon' - j\varepsilon''$ for the composite materials are graphically illustrated in **Figures 2** and **3**. As seen, both the real and imaginary parts showed a decreasing tendency with increasing frequency of electromagnetic radiation. It also becomes evident that both parts were dependent on the content of carbon nanotubes, mainly at low frequencies. The real permittivity of the composite filled with 2.5 phr of $MWCNT$ decreased from 6.3 at 1 MHz to 1.85 at 3 GHz. The increase in filler content to 10 phr resulted

in an increase in real permittivity to 78.2 at 1 MHz. Then, a significant rise of ε' from 78.2 up to 5651.2 occurred by a filler loading increase from 10 to 20 phr at 1 MHz. When the frequency of the electromagnetic radiation increased up to 3 GHz, the real permittivity of the composites filled with 20 phr $MWCNT$ dropped to only 0.16. Similarly, the real permittivity of all MWCNT composites decreased to very low values by increasing the frequency up to 3 GHz. The increasing content of the carbon nanotubes also resulted in an increase in imaginary permittivity at very low frequencies.

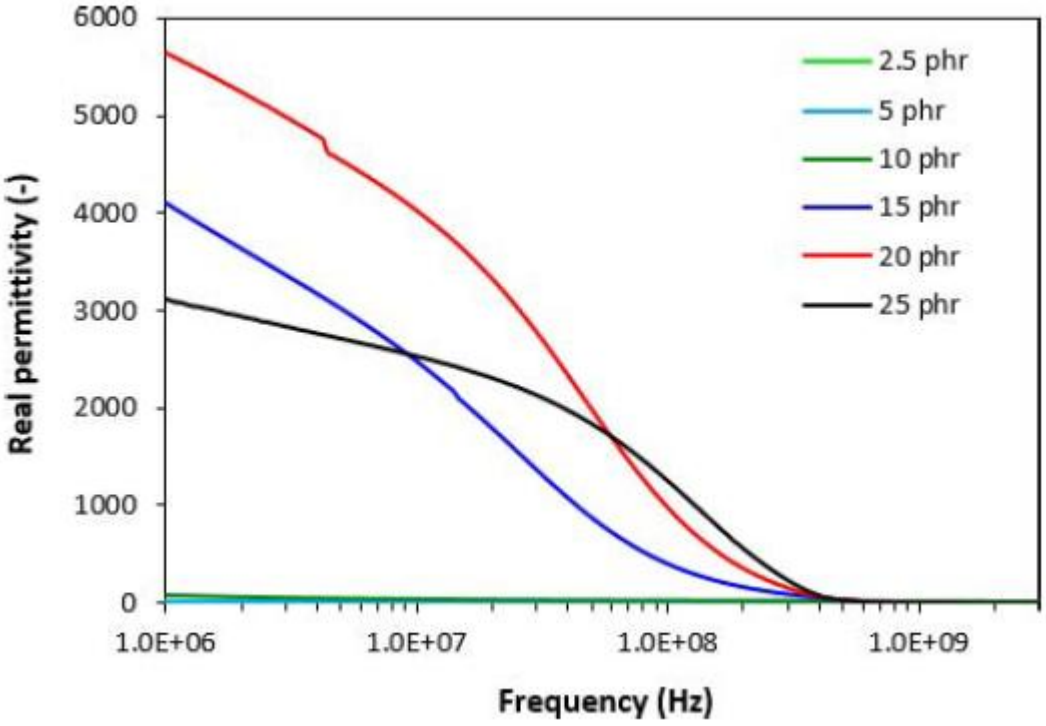

FIG. 2. — Frequency dependences of real part ε' of complex permittivity of composites filled with $MWCNT$.

At 1 MHz, the value of ε'' increased from 2.6 for the composite filled with 2.5 phr of $MWCNT$ up to 3245 for the composite filled with 15 phr of the filler. Then, an outstanding increase in e''occurred by subsequently increasing the degree of filling. The detected value was 46 695 for the composite filled with 20 phr of $MWCNT$ and 83 666 for the maximally filled composite at 1 MHz. Again, the increase in frequency leads to a sharp decrease in imaginary permittivity to very low values.

Real permittivity of composite materials is a measure of the amount of polarization centers and micro-capacitors.22 It is influenced mostly by the polarization (localized charges) inside the composite system and is associated with electrical charge storage within the composite. Polarization of the filler, rubber matrix, and interfacial polarization can occur depending on the frequency range.[23,24]

Defects in the filler structure provide space for polarization centers, while the micro-capacitors are generated by particles or aggregates of the filler, acting as electrodes filled with insulating rubber matrix.[25] Thus, the increase in structural defects and micro-capacitors with the increase in $MWCNT$ loading is responsible for the increase in real permittivity.[26] In addition, the increase in filler loading leads to the reduction of the gap between the MWCNT nanoparticles. This results in an increase in the polarization of the rubber matrix filling the gap between the nanoparticles. A significant increase in real permittivity of composites by increasing the content of $MWCNT$ from 10 phr ($\varepsilon' = 78.2$) to 15 phr ($\varepsilon' = 4113$) is probably caused by reaching the percolation threshold (connecting the filler particles

within the rubber matrix and forming the filler conductive paths). The fact that the real permittivity increased significantly at low frequencies after reaching the percolation threshold suggests that the improvement in permittivity is mainly caused by micro-capacity and polarization of the filler and filler-rubber interfacial charge polarization.[22-24]

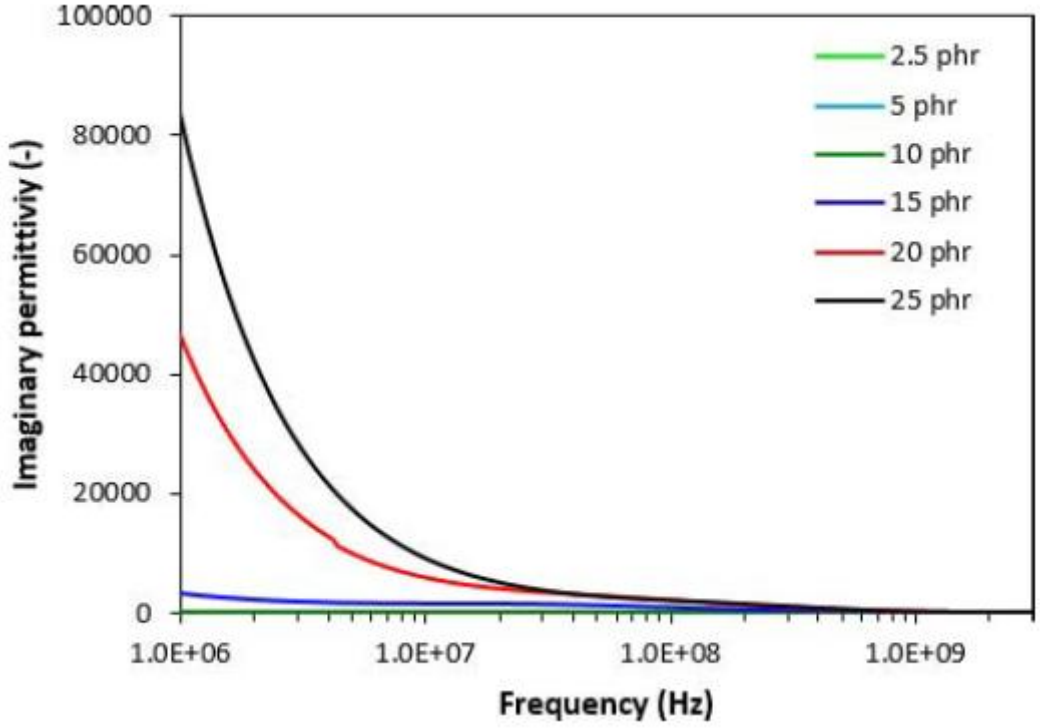

FIG. 3. — Frequency dependences of imaginary part ε'' of complex permittivity of composites filled with $MWCNT$.

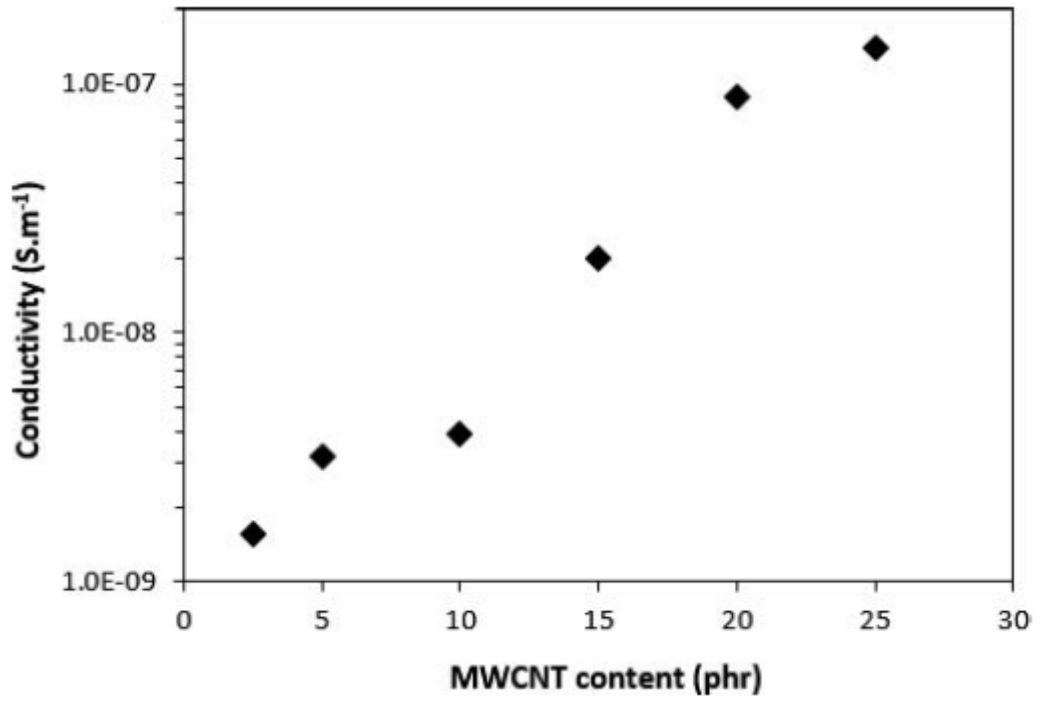

FIG. 4. — Conductivity of composites filled with $MWCNT$.

Imaginary permittivity, which correlates with the dissipation of electrical energy (dielectric loss), is affected by complex phenomena: ionic, electronic, dipole polarization, interfacial polarization, natural resonance, and related relaxation phenomena.[27,28] As already outlined, interfacial and space charge relaxations occur because charge carriers are trapped at the interfaces of the heterogeneous composite system.[27] In general, the increasing amount of conductive filler results in an increase in the number of conductive networks within the composites, which is beneficial for higher imaginary permittivity and consequently for higher values of complex permittivity.[28,29] Conductive filler networks can also act as dissipating mobile charge carriers. The relation between imaginary permittivity and electrical conductivity can be expressed as

$$\varepsilon'' = \sigma/2\pi\varepsilon_0 f \qquad (3)$$

where ε'' is an imaginary part of permittivity, ε' is permittivity of the free space (ε' =8.854 × 10^{-12} F/m), σ is electrical conductivity (S/m), and f is frequency (Hz).

The dependence of electrical conductivity of composites in dependence on $MWCNT$ content is depicted in **Figure 4**. It becomes evident that the conductivity of the composites increased by two orders when the content of the filler increased from 2.5 phr to 25 phr (i.e., from 1.56 × 10^{-9} S/m for the composite filled with 2.5 phr of $MWCNT$ up to 1.4 × 10^{-7} S/m for the maximally filled composite).

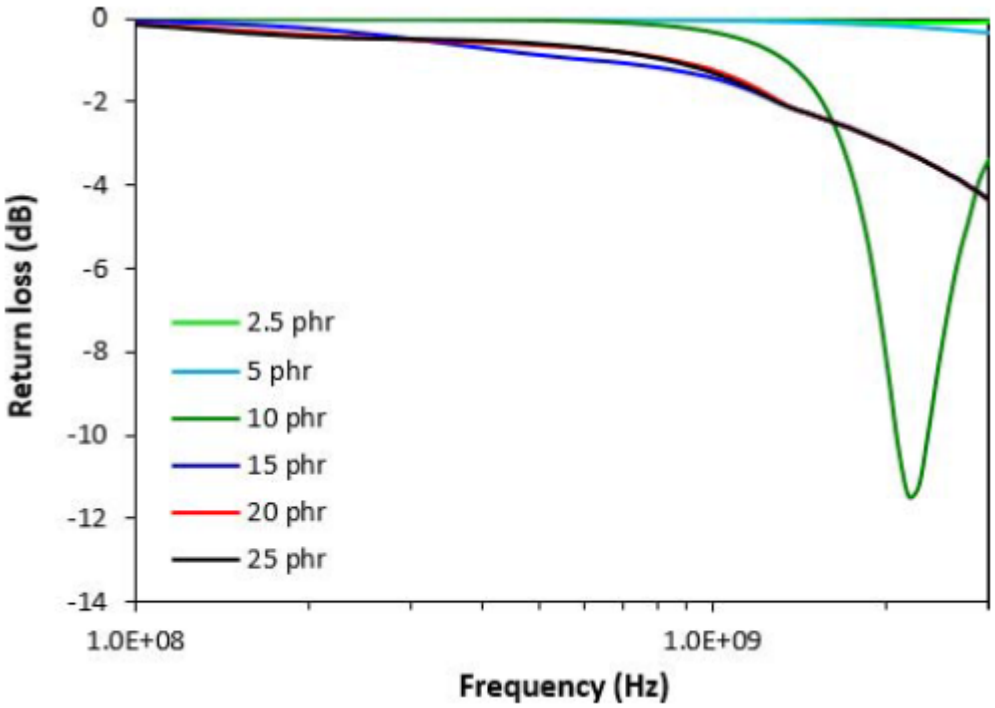

FIG. 5. — Frequency dependences of return loss RL of composites filled with $MWCNT$.

On the other hand, as seen in Eq. 3, the increasing frequency of electromagnetic radiation causes a decrease of imaginary permittivity. Based on the achieved results, it can be stated that high electrical conductivity of carbon nanotubes is responsible for high values of imaginary permittivity and also complex permittivity of composites, mainly at low frequencies.

The absorption shielding efficiency of composite materials was investigated through the determination of return loss in decibels unit. The return loss provides information about the amount of electromagnetic radiation that can be efficiently absorbed by the shield. Scientific studies have reported that materials reaching return loss at —10 dB can absorb 95% of incident electromagnetic radiation. The materials showing a return loss at —20 dB can effectively absorb 99% of EMI.[30-33]

From **Figure 5**, it is possible to observe that composites filled with 2.5 and 5 phr of $MWCNT$ do not provide any absorption shielding ability. On the other hand, the absorption maxima of the composites filled with 15, 20, and 25 phr of $MWCNT$ seem to be reached over the frequency of 3 GHz. As seen in **Figure 5**, only the composite filled with 10 phr of carbon nanotubes exhibited slight absorption shielding ability within the tested frequency range. However, the effective absorption bandwidth at —10 dB is quite narrow and ranges from 2.08 GHz to 2.36 GHz. The absorption maximum of this composite is at —11.5 dB at a frequency of 2.18 GHz. It becomes apparent that composites filled with carbon nanotubes do not provide satisfactory absorption shielding ability in the tested frequency range. The reason can be attributed to extremely high electrical conductivity of carbon nanotubes and thus also very high permittivity. It has been reported that materials with high conductivity are more prone to EMI shielding with dominant reflection mechanism, especially at low frequencies.[34,35] It can be also stated based on the performed experiments that absorption shielding of $MWCNT$-based composites, especially with higher filler loading, might be observed over 3 GHz of incident electromagnetic radiation.

The results obtained from determination of the physical-mechanical properties revealed that modulus M100 (stress at 100% elongation) and the tensile strength of the composites showed a significant increasing tendency with increasing content of carbon nanotubes (**Figure 6**). In comparison with the reference, the application of 25 phr $MWCNT$ resulted in an increase of modulus M100 from 1.4 MPa to greater than 14 MPa. Similarly, the tensile strength of the composites increased from less than 4 MPa for the reference to almost 28 MPa for the maximally filled composite. This remarkable increase clearly points to a high reinforcing effect of carbon nanotubes.

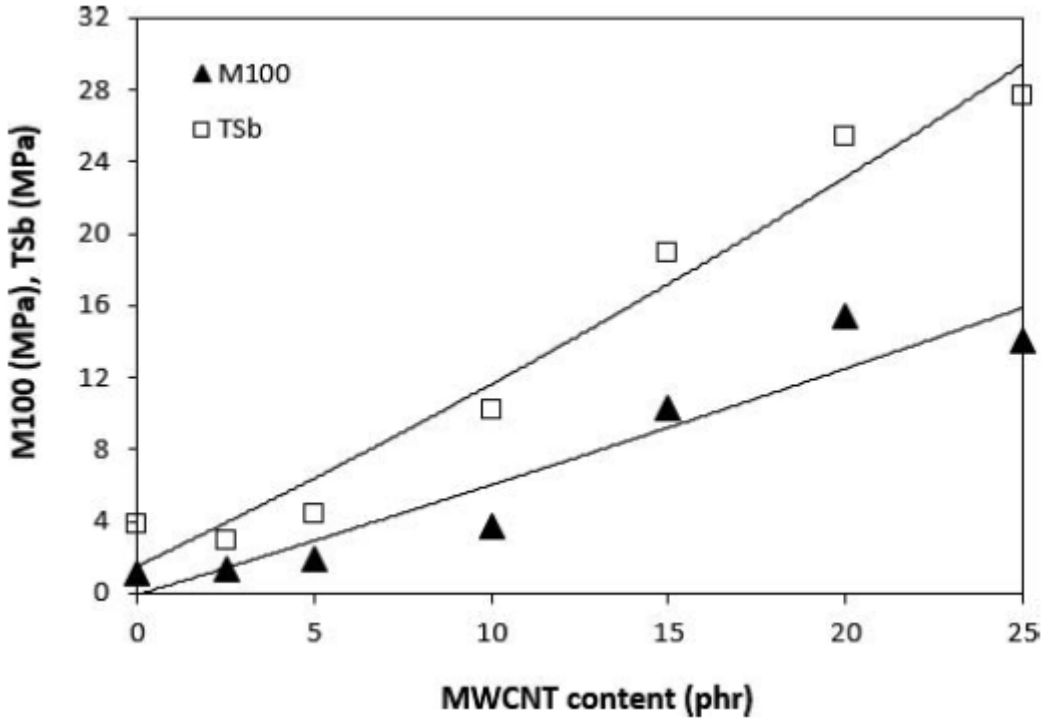

FIG. 6. — Influence of $MWCNT$ content on modulus M100 and tensile strength TSb of composites.

In general, good adhesion and mutual compatibility between the rubber and the filler on the filler-rubber interface with formation of physical or chemical couplings between both components are the main fundamentals of the reinforcing effects of fillers incorporated into the rubber matrix. SEM analysis of the surface fracture of the composites (**Figure 7**a,b) confirmed the presumption showing that the dispersion, homogeneity, and mutual adhesion between carbon nanotubes and rubber matrix is very high, even at ahigh amount of carbon nanotubes in composites.

The results of the study demonstrated that carbon nanotubes reinforce the rubber matrix and contribute to the improvement of physical-mechanical properties and electrical conductivity of composites. However, the EMI absorption shielding ability of composites was observed to be insufficient in the tested frequency range. The main reason can be attributed to the high electrical conductivity and permittivity of carbon nanotubes, which are very important criteria for reflection shielding.

INFLUENCE OF MANGANESE-ZINC FERRITE ON PHYSICAL-MECHANICAL AND SHIELDING CHARACTERISTICS OF COMPOSITES

The second part of the study was aimed at testing the rubber composites with incorporated manganese-zinc ferrite, which was dosed to the rubber formulations in concentration scale ranging from 100 phr to 500 phr. The curing process was again performed at 160 °C. It can be seen from **Figure 8** that the incorporation of magnetic filler resulted in the acceleration of cross-linking process as both the scorch time and the optimum cure time showed a decreasing trend with increasing content of ferrite. Both characteristics decreased by almost 2 min when the content of ferrite increased from 0 up to its maximum content. As already mentioned, the acceleration of the curing process can be attributed to the increase in thermal flow through composites. On the other hand, ferrites are complex compounds of iron oxides with other metal oxides, and their presence in the rubber matrix may have a similar influence as zinc oxide, which serves as a curing activator.

Figure 9 depicts the frequency dependences of real ε' and imaginary ε'' parts of complex permittivity for the composites filled with manganese-zinc ferrite. It becomes obvious that the real part steeply decreases at frequencies up to about 10 MHz and then fluctuates around the constant values. The initial decrease of the real part can be attributed to the semiconductive character of manganese-zinc ferrite. It is also possible to observe that the real permittivity of the composites increased with increasing content of magnetic filler. By increasing the content of ferrite from 100 to 500 phr, the value of s' increased from 18.2 to 73.8 at 1 MHz. The difference in real permittivity became smaller with increasing frequency of electromagnetic radiation. The real part of the composite filled with 100 phr of ferrite decreased to 5.9, whereas the ε'' of the maximally ferrite filled composite decreased to 30.6 at 3 GHz. The imaginary part also first sharply decreases with the increase in frequency. The differences in s'' of composites then became negligible at greater than 1 GHz. When compared with the composites filled with carbon nanotubes, both the real and imaginary permittivity of the composites with manganese-zinc ferrite provide much lower values. The achieved changes in frequency dependences of complex permittivity may be attributed to various polarization mechanisms originating in the ferrite as well as rubber matrix due to their dielectric character (mainly interfacial polarization caused by space charges, which accumulate at the boundaries of the filler-rubber interface).

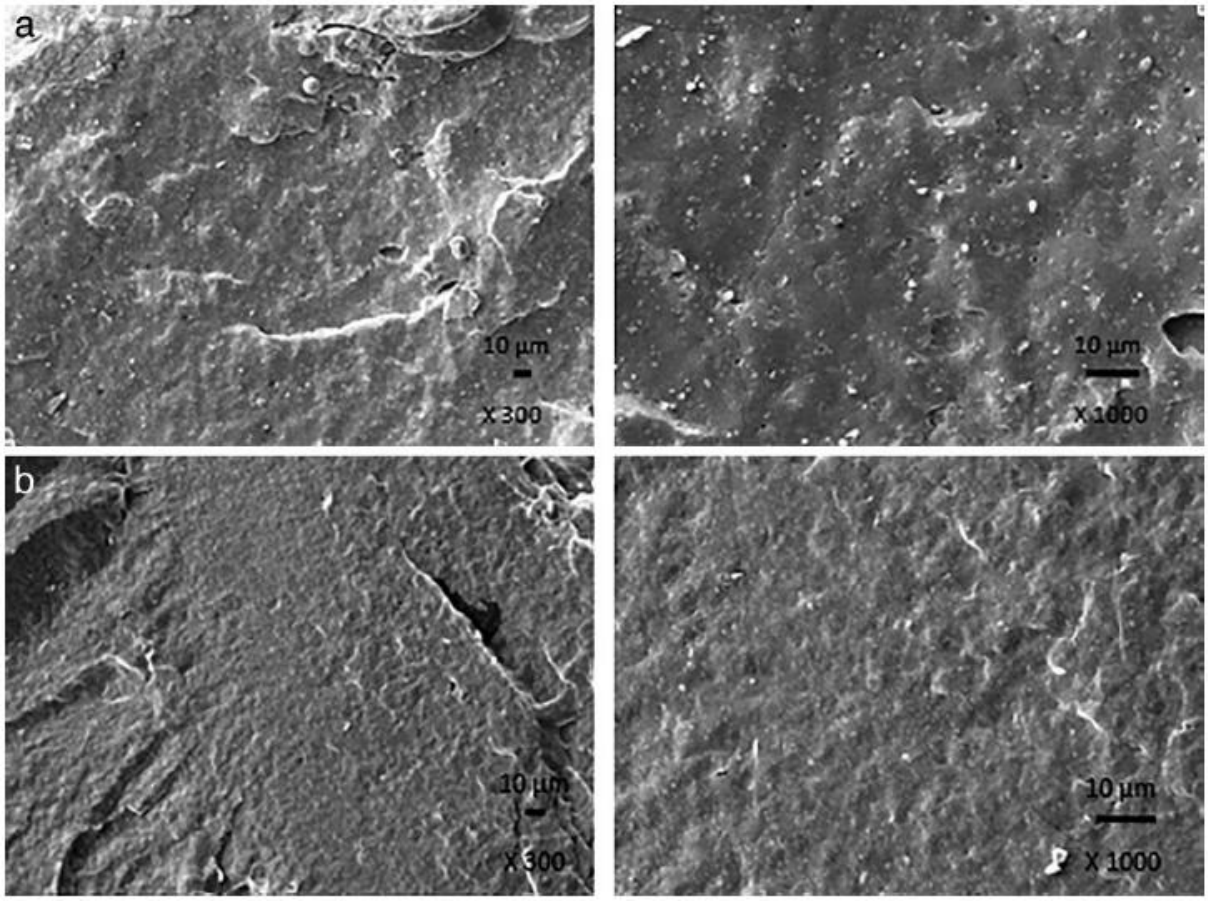

FIG. 7. — (a) SEM images of composite filled with 5 phr of $MWCNT$. (b) SEM images of composite filled with 25 phr of $MWCNT$.

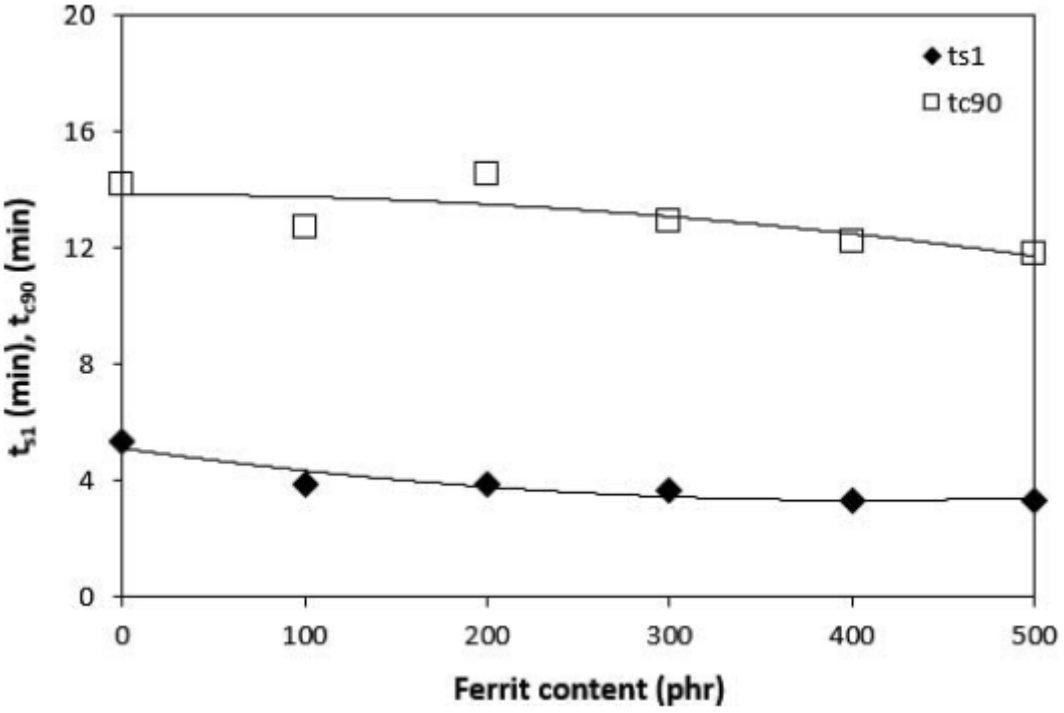

FIG. 8. — Influence of ferrite content on scorch time t_{s1} and optimum cure time t_{c90} of rubber compounds.

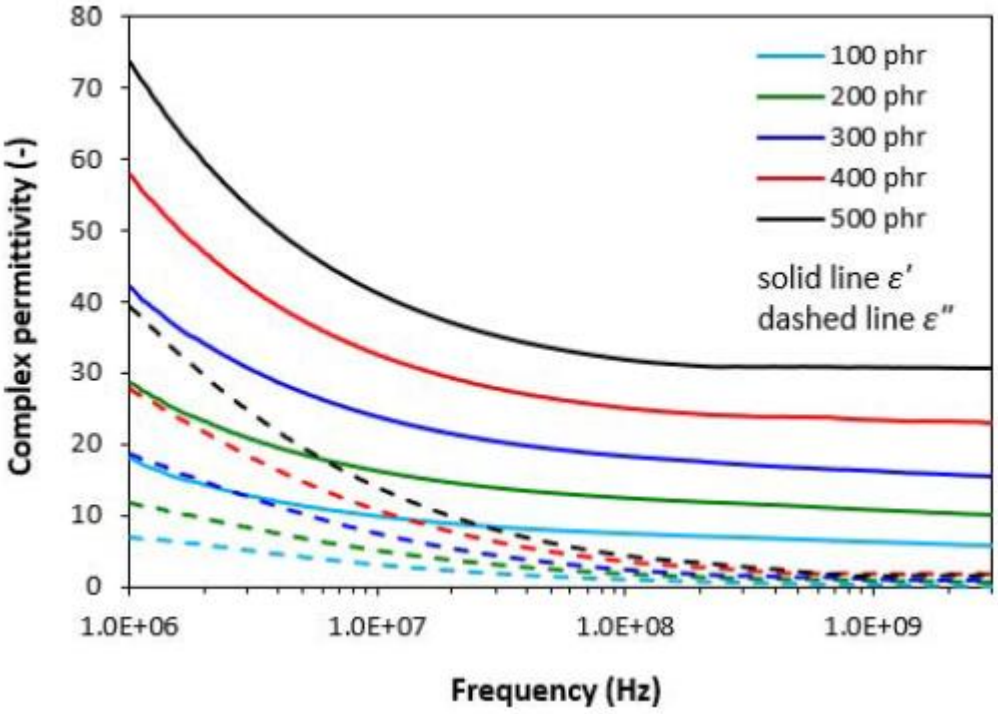

FIG. 9. — Frequency dependences of real ε' and imaginary ε'' parts of complex permittivity of composites filled with ferrite.

From frequency dependences of return loss of composites (**Figure 10**), it becomes apparent that all composites containing ≥200 phr of filler provide satisfactory absorption shielding efficiency in the tested frequency range. As also seen, the absorption maxima and absorption shielding efficiency of the composites move to lower frequencies with increasing content of magnetic filler. The best absorption shielding material can be considered to be the composite containing 200 phr of manganese-zinc ferrite, because it exhibited return loss at —10 dB and —20 dB in the widest frequency range (i.e., from 1.5 GHz to 2.7 GHz at—10 dB and from 1.85 GHz to 2.2 GHz at—20 dB). The absorption maximum of this composite shield is at —48 dB at a frequency of 2 GHz of the incident electromagnetic radiation. The composite filled with 400 phr of ferrite exhibited lower absorption maximum (—60 dB) but also a lower frequency range with effective absorption of EMI (return loss at —10 dB in the frequency range of 0.6-0.98 GHz and return loss at —20 dB in the frequency range of only 0.72— 0.83 GHz). The maximally filled composite was found to have the highest absorption maximum and the lowest effective absorption bandwidth. The electromagnetic absorption characteristics (minimum value of return loss RL_{min} at a matching frequency f_m, matching frequency f_m, bandwidth Δf for return loss at—10 and at —20 dB) are presented in **Table III**. The achieved results demonstrated that composites filled with manganese-zinc ferrite can be used as effective EMI shields at frequencies greater than 500 MHz. It becomes apparent that, on one hand, with the increase of ferrite content, the efficient absorption shielding ability of composites shifts to lower frequencies of electromagnetic radiation. On the other hand, based on narrower absorption peaks of composites filled with higher ferrite content, it can be stated that absorption shielding of those composites is lower when compared with composites with lower ferrite content. The reason for this can be attributed to the increase in electrical conductivity of composites with increase in filler loading. From **Figure 11**, it is apparent that the conductivity of the composites increased by almost three orders via an increase in ferrite content from 100 to 500 phr, despite the fact that ferrite is a semiconductive filler.

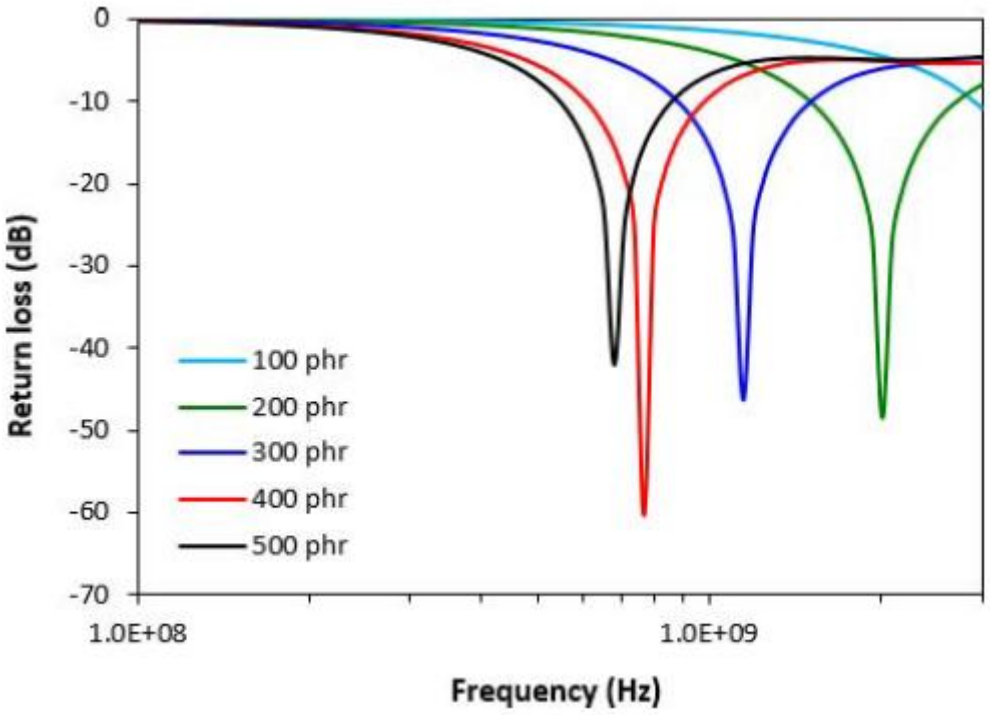

FIG. 10. — Frequency dependences of return loss RL of composites filled with ferrite.

Thus, it is believed that composites with greater ferrite content are also more prone to shielding by reflection. When compared with composites filled with carbon nanotubes, composites filled with ferrite provide much lower values of permittivity, which still enable the absorption shielding efficiency of these composites. Another difference in contrast to nonmagnetic carbon nanotubes is the presence of magnetic dipoles in magnetic soft ferrites. It has been demonstrated that materials possessing magnetic dipoles are suitable candidates for EMI shielding by absorption.[36-38]

The physical-mechanical properties of the composites were also tested, and the influence of the magnetic filler content on tensile strength and modulus M100 of the composite systems is illustrated graphically in **Figure 12**. As shown, both characteristics exhibited a decreasing trend with increasing content of ferrite, which indicates that manganese-zinc ferrite behaves as an inactive filler in the rubber matrix.

Table III Electromagnetic Absorption Parameters for the Composites Filled with Manganese-Zinc Ferrite

Ferrite content, phr	RL_{min}, dB	f_m, MHz	Δf for RL at −10 dB, MHz	Δf for RL at −20 dB, MHz
100				
200	−48	2010	1220	370
300	−46	1148	630	188
400	−60	769	380	115
500	−42	682	310	103

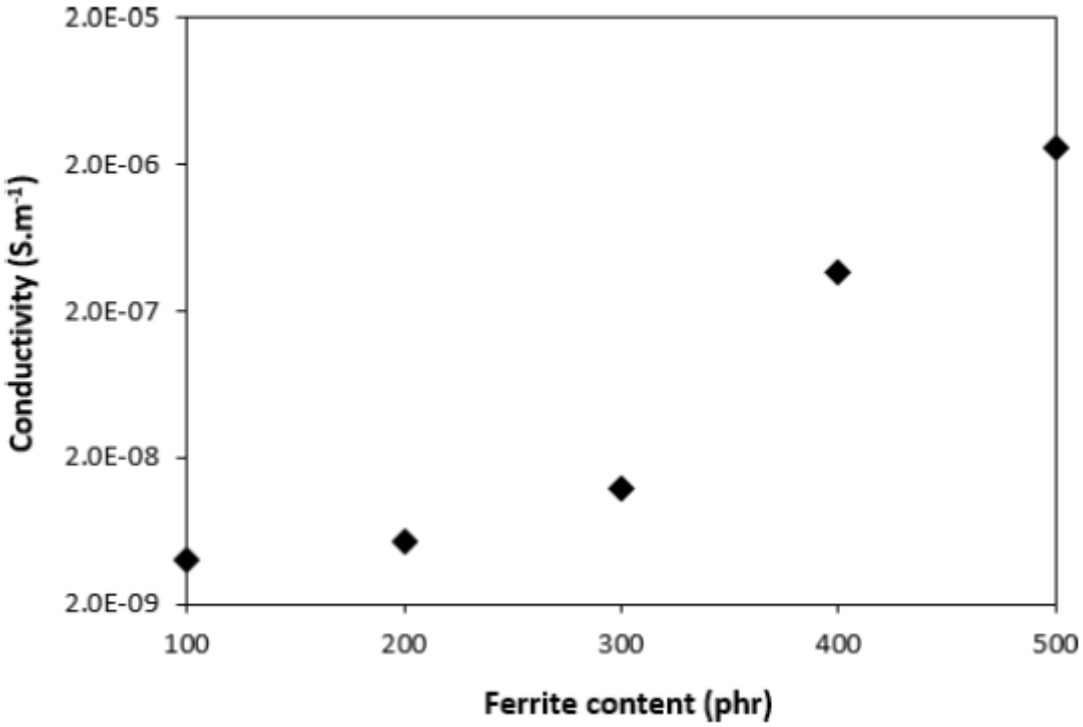

FIG. 11. — Conductivity of composites filled with ferrite.

A high level of filler loading and mainly poor compatibility and adhesion between the rubber and the filler on the filler-rubber interface seem to be the main reasons for the deterioration of the physical-mechanical characteristics. SEM analysis of the surface fractures of the composites clearly demonstrated that the adhesion between the filler and the rubber was weak with existence of voids and cavities on the filler-rubber interface (**Figure 13**a-c). Those inhomogeneities and voids were likely caused during the fracturing of the composites for their preparation for SEM analysis and dropping out poorly bonded ferrite particles. It also becomes apparent from the SEM images that the higher the amount of ferrite in the composites, the higher the agglomeration of filler particles, which also contributes to the deterioration of physical-mechanical properties. From the graphical dependence of the complex viscosity on shear rate (**Figure 14**), it is obvious that the presence of magnetic filler in the matrix affects the viscosity of the rubber compounds. As seen, the higher the amount of ferrite, the higher the viscosity. The differences in complex viscosity are more visible at lower shear rates. With increasing shear rate, the differences in the complex viscosity of the rubber systems depending on ferrite content become less visible. The decrease in complex viscosity with the increase in shear stress points toward the pseudo-plastic behavior of the rubber compounds. Generally, lower shear rates are generated with the compounding of elastomer compounds in kneading machines, which means that with a higher viscosity, the mixing and compounding could be more difficult. However, it must be stated that the processing of the rubber compounds was still possible under the given mixing conditions.

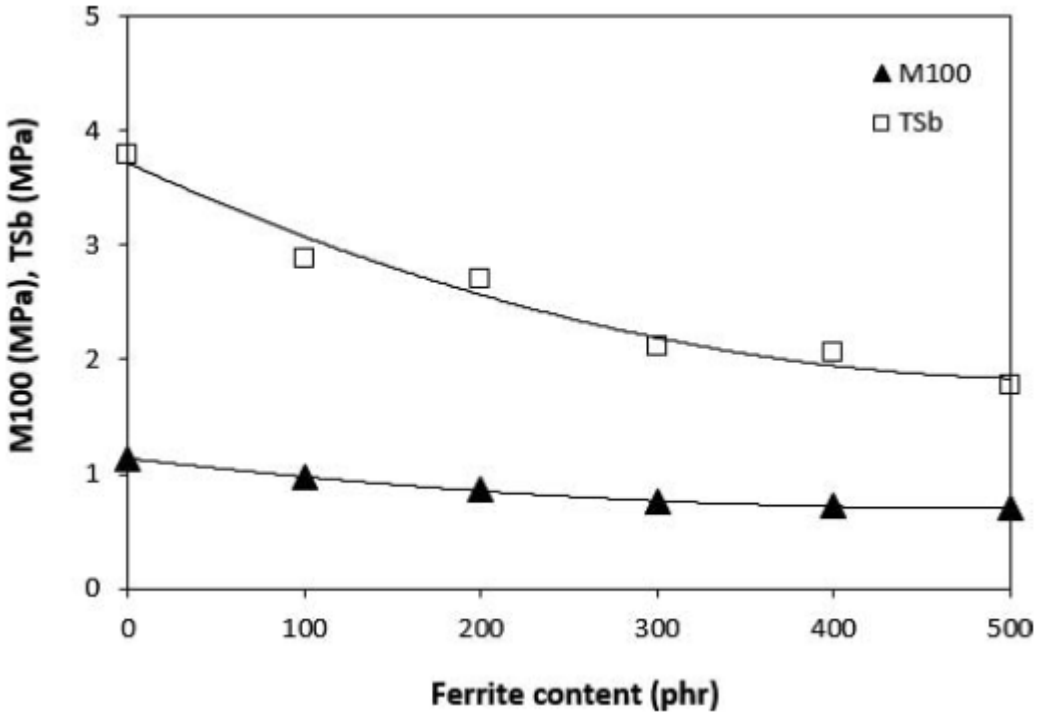

FIG. 12. — Influence of ferrite content on modulus M100 and tensile strength TSb of composites.

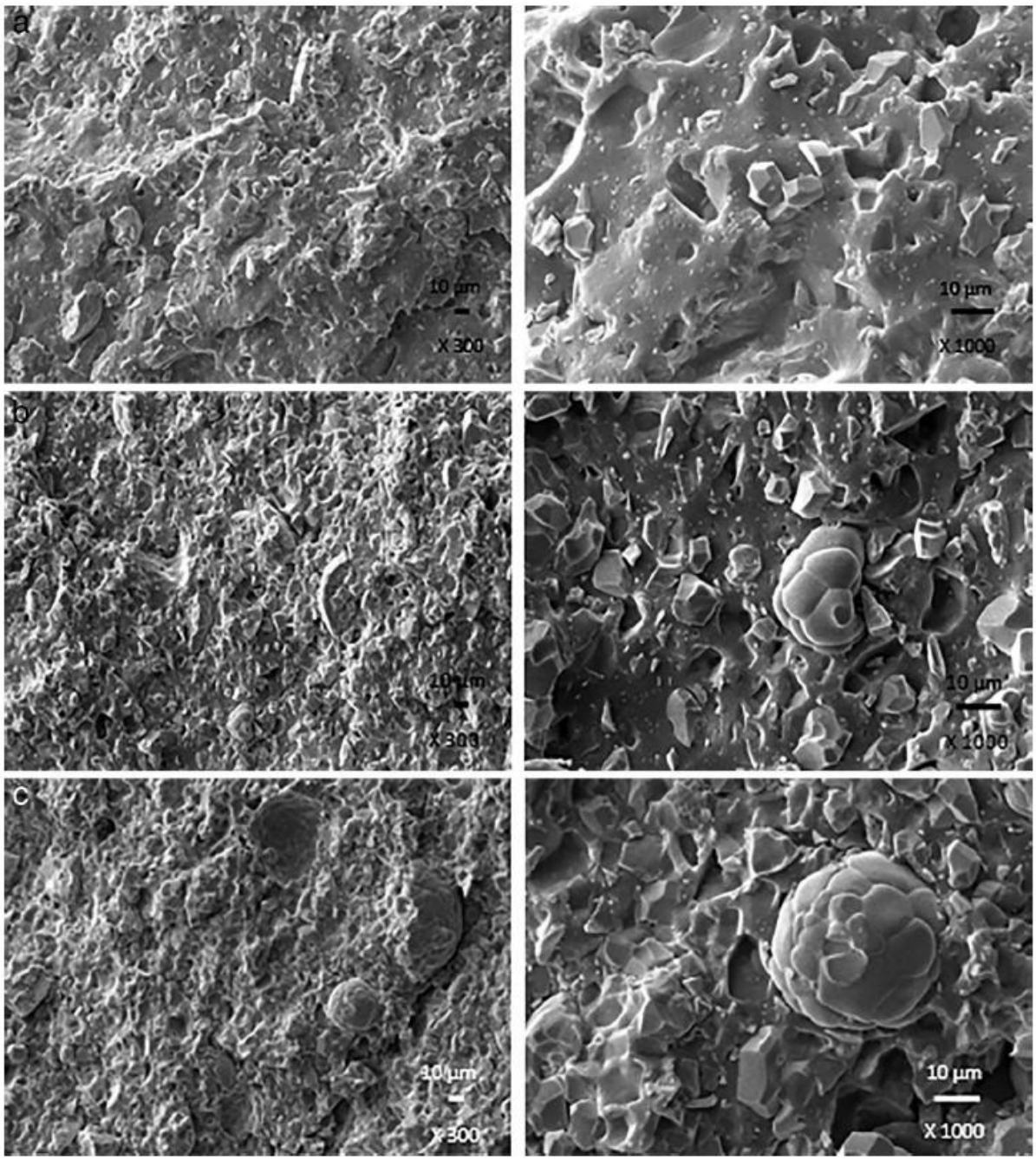

FIG. 13. — (a) SEM images of composite filled with 100 phr of ferrite. (b) SEM images of composite filled with 300 phr of ferrite. (c) SEM images of composite filled with 500 phr of ferrite.

The application of manganese-zinc ferrite into an NBR-based matrix was revealed to lead to the preparation of rubber magnetic composites with EMI shielding effectiveness. The main benefit of these composites is the ability to shield electromagnetic radiation by absorption mechanisms. On the other hand, physical-mechanical properties such as tensile strength and the moduli of composites deteriorated, which could hinder the utilization of these materials in industrial applications.

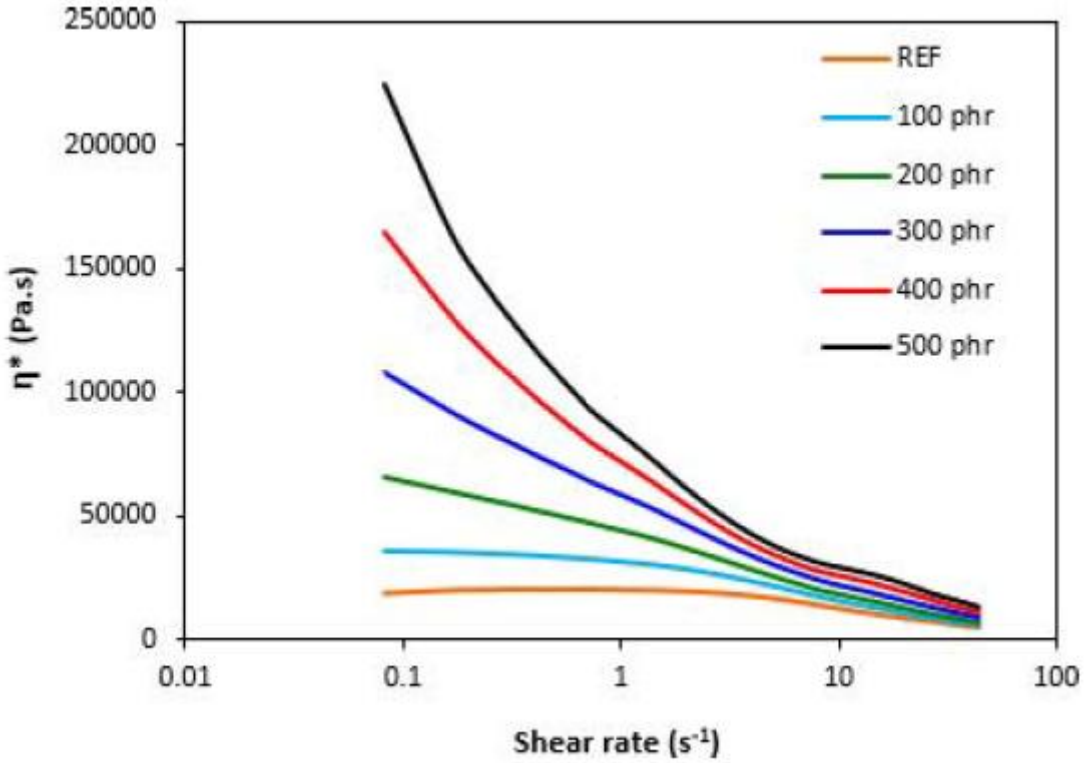

FIG. 14. — Influence of ferrite content on complex viscosity of rubber compounds.

INFLUENCE OF THE COMBINATION OF CARBON NANOTUBES AND MANGANESE-ZINC FERRITE ON PHYSICAL-MECHANICAL AND SHIELDING CHARACTERISTICS OF COMPOSITES

In the third part of the study, carbon nanotubes were combined with magnetic filler to prepare rubber composites. The content of the carbon nanotubes was kept constant in all composites (5 phr), whereas manganese-zinc ferrite was dosed to the rubber formulations in an amount ranging from 100 to 500 phr. Because carbon nanotubes are one of the strongest and stiffest materials with an excellent reinforcing effect when incorporated into polymer matrices, in general, only low amounts are required to achieve the high tensile and tear strength characteristics of composites. Therefore, 5 phr of $MWCNT$ was chosen as the constant amount for the subsequent experiments.

As shown in **Figure 15**, with the increasing content of magnetic filler in the composites filled with the combination fillers, the scorch time was shortened. When compared with the reference composite filled with only $MWCNT$, the incorporation of 300 phr of ferrite also resulted in a decrease in the optimum cure time in about 4.5 min (decreasing from 17.5 min for the reference to 13 min for the composite filled with 300 phr of ferrite). The application of ferrite over 300 phr then caused an increase in the optimum cure time. It can be seen that the maximally filled rubber compound required almost the same time for optimum curing as the reference sample did.

In the graphical illustrations, the physical-mechanical properties of the composites filled with a combination of carbon nanotubes and ferrite are compared with the equivalent characteristics of the composites filled only with magnetic filler. From **Figures 16** and **17**, it can be seen that both modulus M100 and the tensile strength of the composites filled with a combination of $MWCNT$ and ferrite were higher when compared with the corresponding composites filled only with magnetic filler.

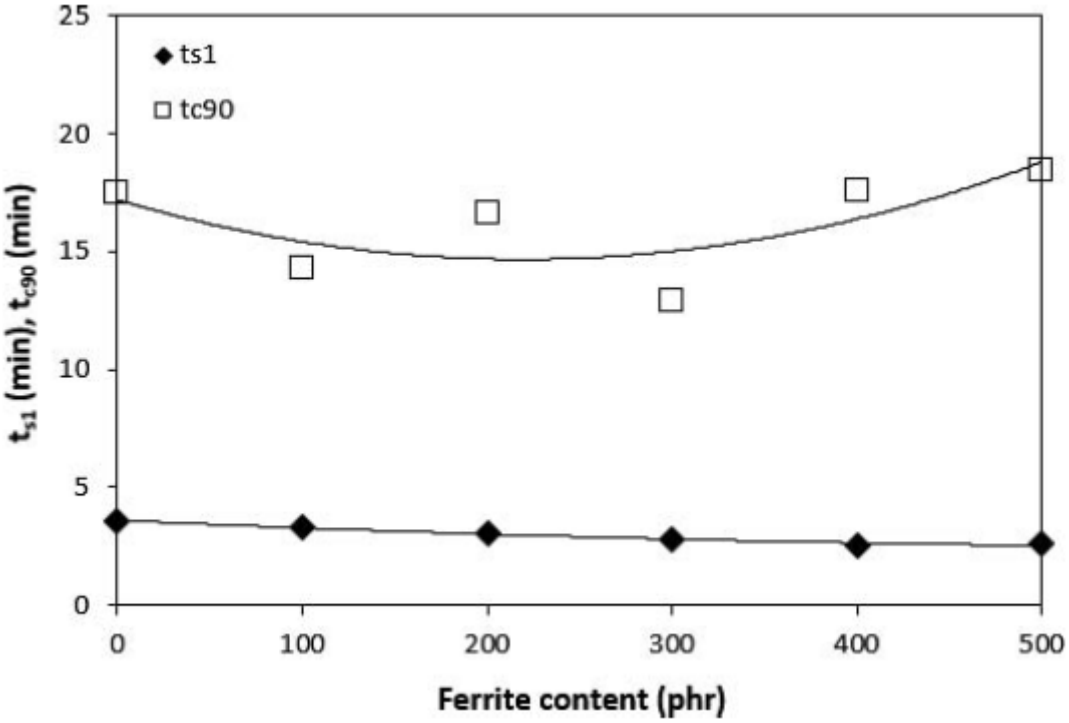

FIG. 15. — Influence of ferrite content on scorch time t_{s1} and optimum cure time t_{c90} of hybrid $MWCNT$/ferrite rubber compounds.

It can be stated that the application of carbon nanotubes leads to the reinforcement of the rubber matrix and thus to an increase in the physical-mechanical properties of the composites. As also shown in **Figures 16** and **17**, the lowest difference in both characteristics was recorded for the reference unfilled sample and composite filled with 5 phr of $MWCNT$. The application of 100 phr of ferrite in the composites filled with a combination of fillers resulted in an increase of both modulus and tensile strength. This seems to be very surprising and points to some synergistic effect of the combination of both fillers. With the next increase in the magnetic filler in the hybrid composites, modulus M100 and tensile strength showed a decreasing trend. However, the values of both parameters for hybrid composites were still higher when compared with the composites filled only with ferrite. SEM analysis of the composites-filled combination of fillers (**Figure 18**a-c) revealed that the dispersion of fillers, mainly ferrite in hybrid composites, was better in comparison with composites filled only with magnetic filler, mainly at lower ferrite content (**Figure 13**). The presence of $MWCNT$ results in a higher viscosity of the rubber matrix (**Figure 19**) and thus also higher shear stress during compounding. Higher shear stress subsequently facilitates dispersion and distribution of ferrite within the rubber matrix. A higher dispersion state of ferrite particles in the rubber matrix could also contribute to enhanced physical-mechanical properties of hybrid composites. As also seen in **Figure 19**, the viscosity of the $MWCNT$/ferrite composites increased with increasing content of magnetic filler. Although the higher viscosity of the rubber matrix generates higher shear stress during compounding that leads to better dispersion mixing, a viscosity that is too high might be difficult for the overall processing of rubber compounds. Thus, it is believed that the very high viscosity of the rubber compounds with high ferrite content could play a negative role in their compounding, which can also be deduced from the SEM images of hybrid composites with high ferrite content showing some agglomeration of ferrite particles. This agglomeration could be also the reason for the worsening of mechanical properties for highly filled composites.

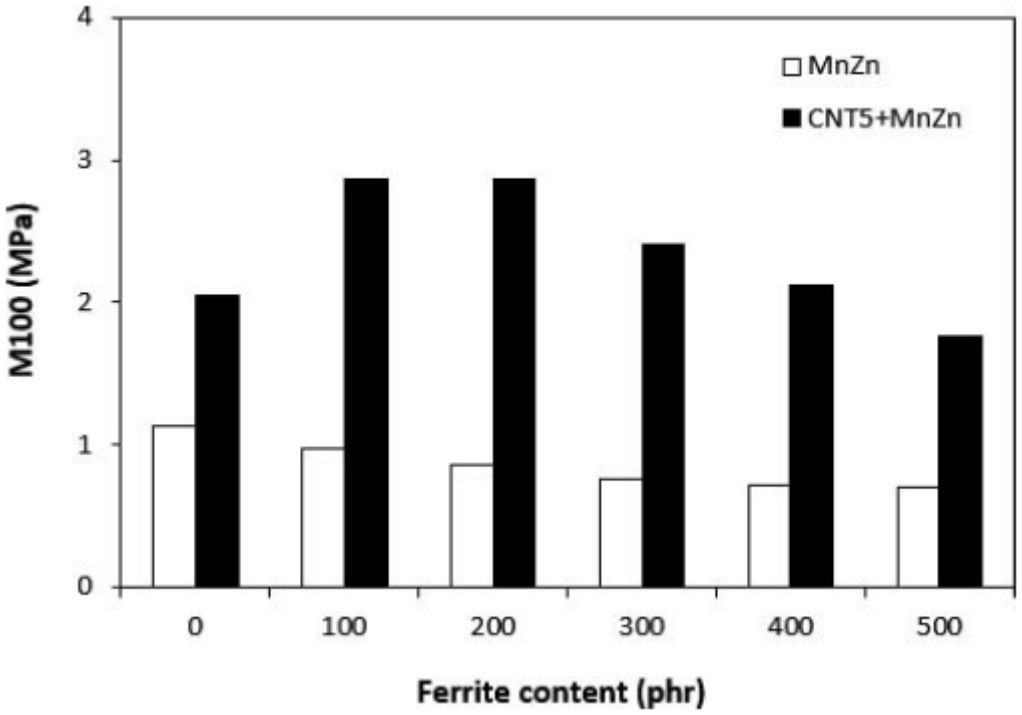

FIG. 16. — Influence of ferrite content on modulus M100 of hybrid $MWCNT$/ferrite composites.

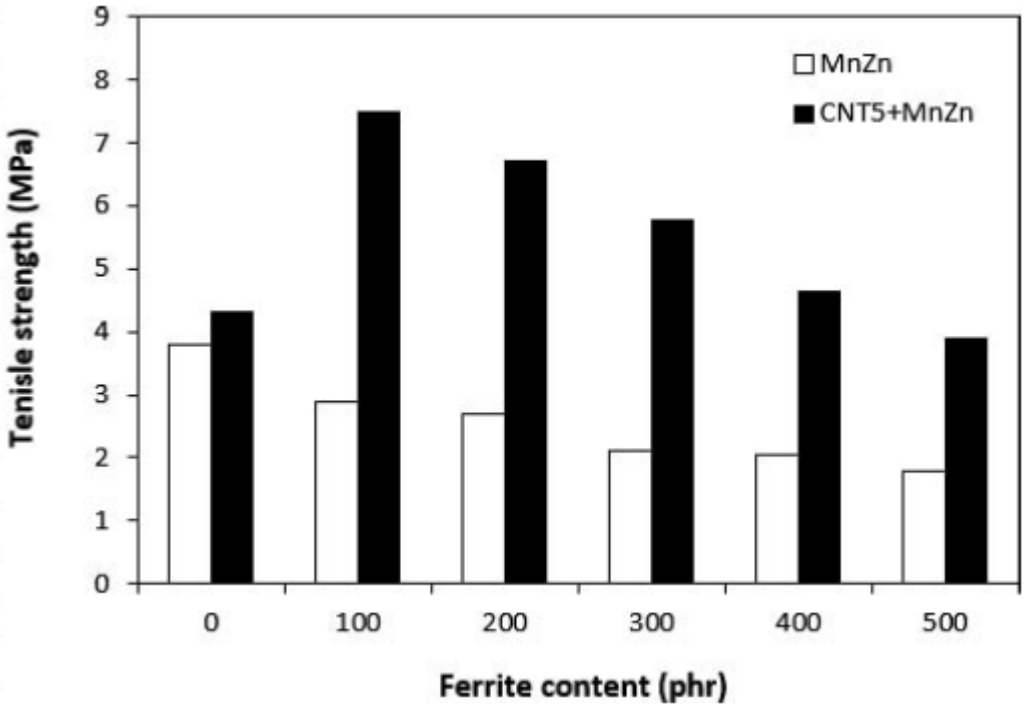

FIG. 17. — Influence of ferrite content on tensile strength of hybrid $MWCNT$/ferrite composites.

From **Figure 20**, it becomes obvious that both the real ε' and imaginary ε'' parts of complex permittivity of hybrid $MWCNT$/ferrite composites showed a sharp decreasing trend with increasing frequency.

When compared with composite filled only with 5 phr of $MWCNT$, the incorporation of 100 phr ferrite led to the increase in real permittivity from 23.2 up to 371.1 at 1 MHz. The increasing content of ferrite in the hybrid composites resulted in an increase in real permittivity of up to 200 phr of ferrite at 1 MHz ($\varepsilon' = 1147$ for the composite filled with 5 phr of $MWCNT$ and 200 phr of ferrite). Then, the real permittivity decreased slightly with the next increasing content of magnetic filler at 1 MHz ($\varepsilon' = 966$ for the composite filled with 5 phr of $MWCNT$ and 500 phr of ferrite). Subsequently, the real permittivity of the hybrid composites decreased to very low values by increasing the frequency from 1 MHz to 3 GHz. For example, the real permittivity of the composites decreased to 17.1 or 0.1, respectively, by increasing the content of ferrite from 100 phr to 500 phr at 3 GHz. The initial decrease in real permittivity with frequency may be attributed to the semiconductive character of manganese-zinc ferrite and the conductive character of carbon nanotubes. The similar trend can also be observed in the frequency dependences of imaginary permittivity. **Figure 20** shows that values of imaginary part ε'' are very similar to the real permittivity ε' of the corresponding composites in the whole tested frequency range. The incorporation of 100 phr of ferrite resulted in an increase in imaginary permittivity of more than 430 at 1 MHz (from $\varepsilon'' = 8.8$ for the composite filled with 5 phr of $MWCNT$ up to $\varepsilon'' = 439.1$ for the composite filled with 5 phr of MWCNT and 100 phr of ferrite). The imaginary permittivity of the hybrid composite filled with 100 phr ferrite dropped to 7.3 by increasing the electromagnetic radiation frequency up to 3 GHz. The imaginary permittivity of the maximally filled composite was reduced from 807.1 at 1 MHz to 1.5 at 3 GHz. When comparing the complex permittivity of composites filled only with manganese-zinc ferrite (**Figure 9**) and complex permittivity of the hybrid $MWCNT$/ferrite composites (**Figure 20**), it becomes apparent thatboth the real and imaginary permittivity of the hybrid composites are much higher when compared with the corresponding ferrite-filled composites. The highervalues of the complex permittivity of the hybrid composites can be attributed to the presence of conductive filler-carbon nanotubes.

As already outlined, the real part of permittivity is related to the electrical charge storage and mainly associated with the amount of polarization in the material, whereas the imaginary part of permittivity is related to the loss in energy (dielectric loss). The presence of a high amount of interfaces in the composites paves the way for interfacial polarization, which occurs on carbon nanotube particles with relatively high conductivity. This leads to the accumulation of charges at the interfaces and the generation of dipoles on semiconducting ferrite particles (**Figure 21**). Thus, the interfacial polarization and associated space charge relaxation processes contribute to the EMI shielding ability.[39,40] In hybrid $MWCNT$/ferrite rubber composites, manganese-zinc ferrite acts as a polarized center in the presence of electromagnetic radiation.

The frequency dependences of return loss for hybrid $MWCNT$/ferrite composites are graphically illustrated in **Figure 22**. It is shown that the composite filled only with 5 phr of carbon nanotubes and hybrid composites containing 5 phr of carbon black and ≥200 phr of ferrite do not provide any absorption shielding ability, because they do not reach return loss of at least —10 dB. The reason for this is the high electrical conductivity and complex permittivity of composites filled with a combination of $MWCNT$ and ferrite. As previously outlined, materials with high electrical conductivity are suitable candidates for electromagnetic field shielding applications based on reflection. The absorption shielding performance was recorded only for the composite filled with 5 phr of $MWCNT$ and 100 phr of ferrite. However, the effective absorption bandwidth of this composite at —10 dB ranged only from 1.14 to 1.39 GHz. The absorption maximum of this composite was at —11.2 dB at frequency 1.24 GHz of the incident electromagnetic radiation.

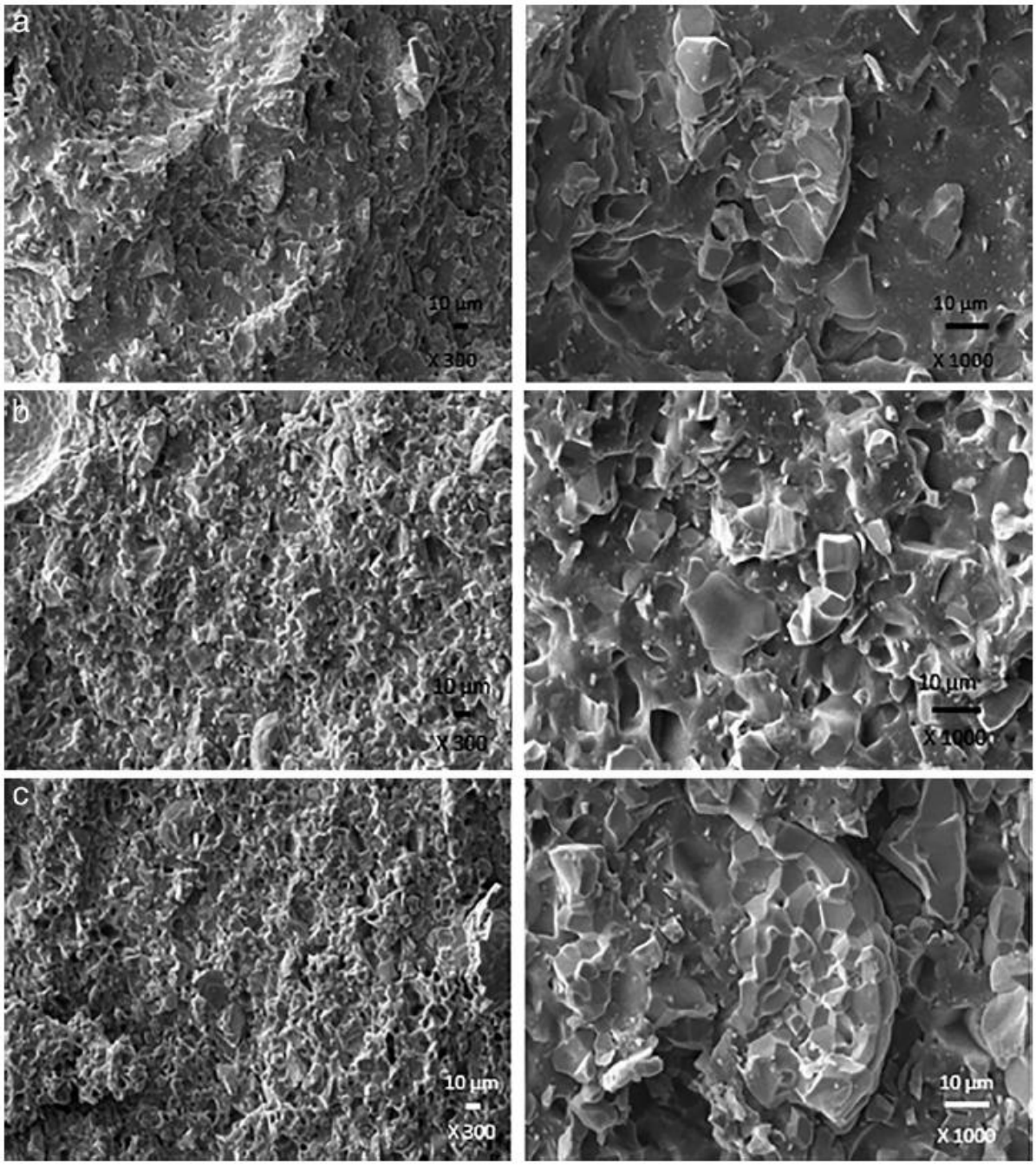

FIG. 18. — (a) SEM images of composite filled with 5 phr of $MWCNT$ and 100 phr of ferrite. (b) SEM images of composite filled with 5 phr of $MWCNT$ and 300 phr of ferrite. (c) SEM images of composite filled with 5 phr of $MWCNT$ and 500phr of ferrite.

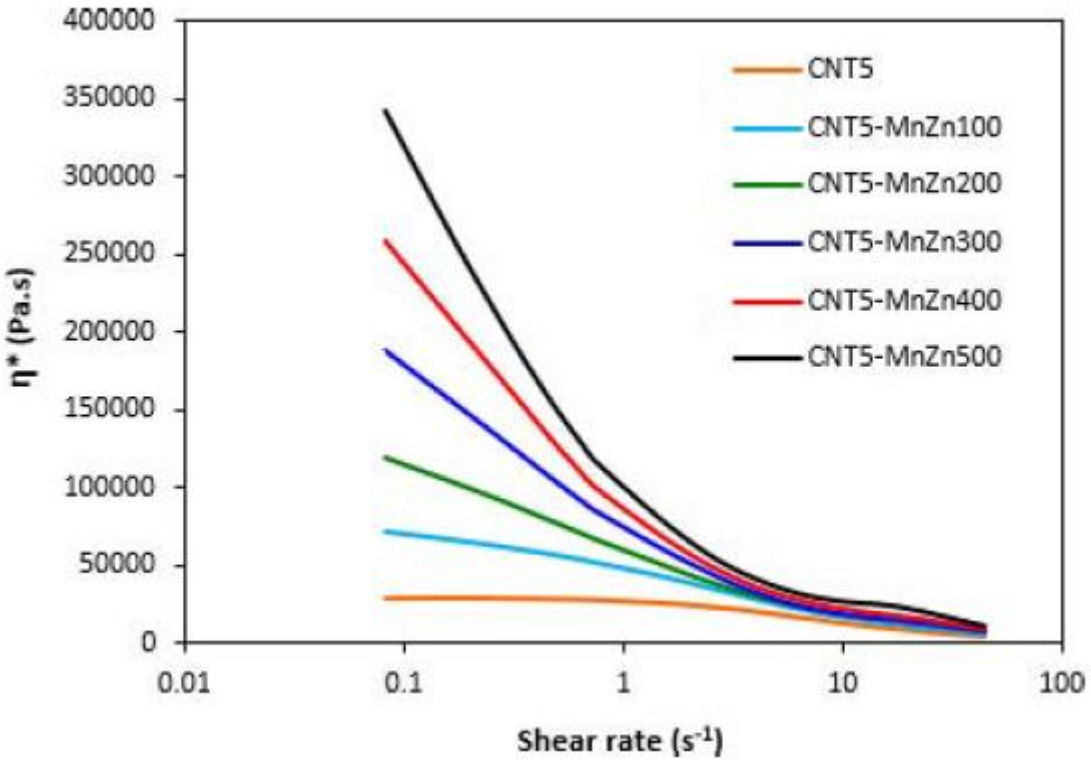

FIG. 19. — Influence of ferrite content on complex viscosity of hybrid $MWCNT$/ferrite rubber compounds.

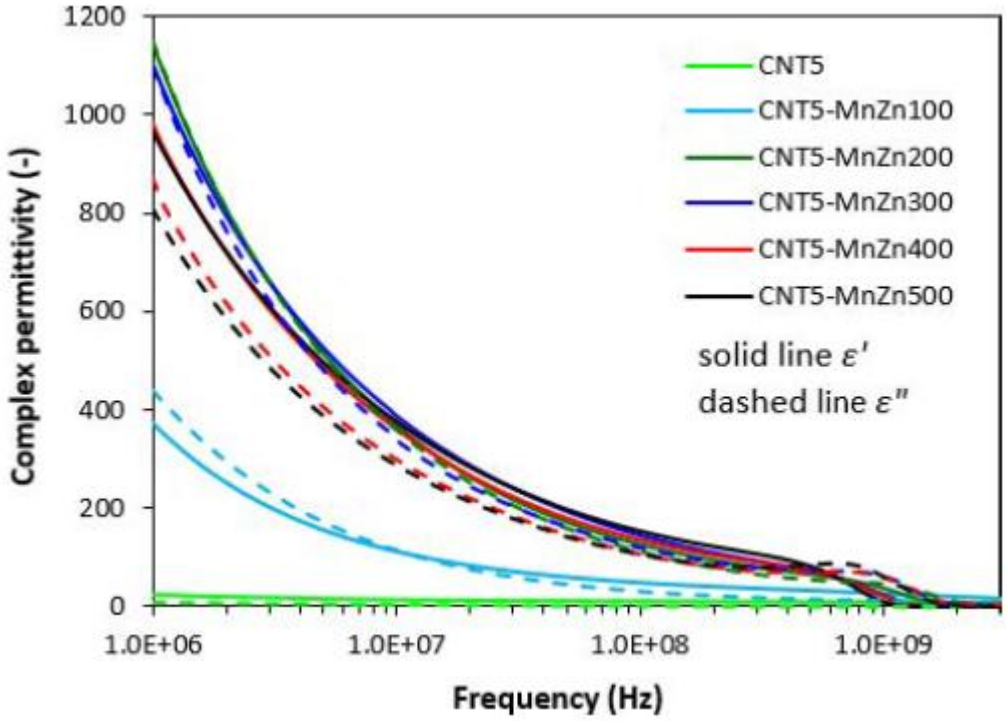

FIG. 20. — Frequency dependences of real ε' and imaginaryε'' parts of complex permittivity of hybrid $MWCNT$/ferrite composites.

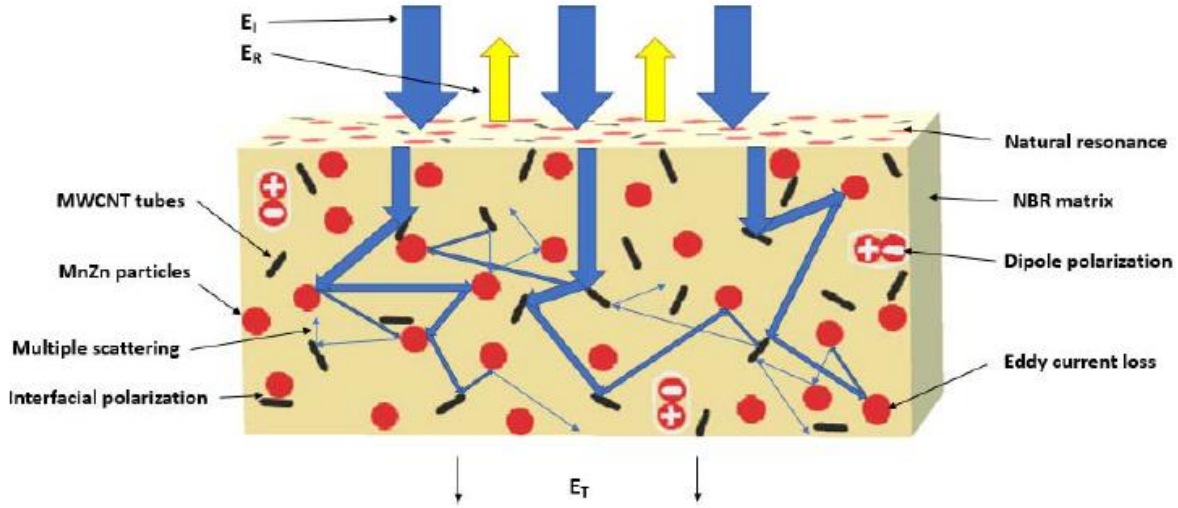

FIG. 21. — Schematic illustration of EMI shielding mechanisms for hybrid $MWCNT$/ferrite composites.

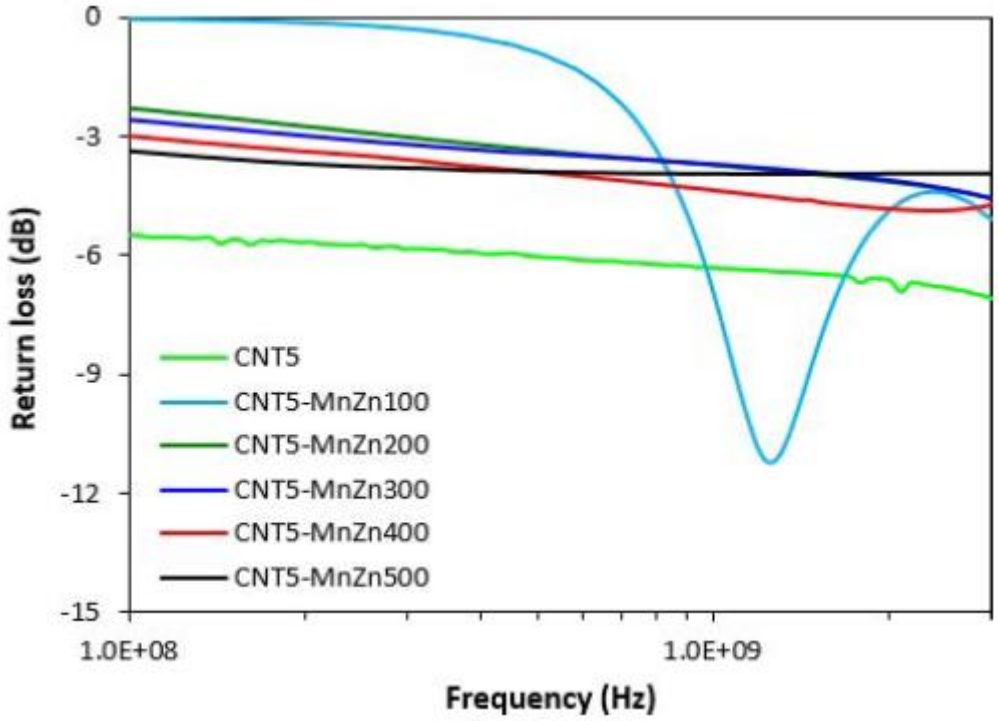

FIG. 22. — Frequency dependences of return loss RL of hybrid $MWCNT$/ferrite composites.

CONCLUSION

This article focused on the investigation of carbon nanotubes, manganese-zinc ferrite, and the combination of carbon nanotubes with ferrite on electromagnetic absorption shielding properties and physical-mechanical characteristics of NBR-based composites.

The results revealed that composites filled with carbon nanotubes exhibited excellent physical-mechanical properties. However, because of the high value of conductivity and permittivity, their EMI absorption shielding was insufficient within the frequency range of 1 MHz to 3 GHz. On the other hand, composites with incorporated manganese-zinc ferrite can be applied as efficient EMI shielding

materials with absorption-dominated shielding characteristics over the tested frequency range. The combination of carbon nanotubes and ferrite resulted in higher viscosity of the rubber matrix and higher shear stress during compounding, which facilitated better dispersion of magnetic filler within the rubber composites. On other hand, conductive carbon nanotubes contributed to various polarization mechanisms, charge storage, and related associated space charge relaxation phenomena within the rubber matrix, which was reflected in the increase in complex permittivity. Because the conductivity and complex permittivity of the hybrid composites were very high, the absorption shielding was low, suggesting that the dominant shielding mechanism of excellent conductive materials is based on the reflection of EMI.

REFERENCES

[1]M. E. Abubaker Ali and M. M. Ahmed, Am. J. Eng. Res. **6**, 8 (2017).

[2]C. E. Okechukwu, Adv. Hum. Biol. **10**, 6 (2020).

[3]P. Kumar, A. Kumar, K. Y. Cho, T. K. Das, and V. Sudarsan, AIPAdv. **7**, 015103 (2017).

[4]A. Sanida, G. S. Stavropoulos, T. Speliotis, and G. C. Psarras, Materials **12**, 3015 (2019).

[5]E. Ušák, M. Ušáková, R. Dosoudil, M. Šoka, and E. Dobročka, $AIP\ Adv.$ **8**, 047805 (2018).

[6]R. S. Mane and V. V. Jadhav, ''Types, Synthesis Methods and Applications of Ferrites,'' in $Spinel\ Ferrite\ Nanostructures\ for\ Energy\ Storage\ Devices$, Elsevier, Philadelphia, 2020.

[7]R. H. Kadam, R. B. Borade, M. L. Lane, D. R. Mane, K. M. Batoo, and S. E. Shirsath, $RSC\ Adv.$ **10**, 27911 (2020).

[8]K. P. Jeong, S. W. Yang, J. H. Choi, and J. G. Kim, $Metals\ Mater.Int.$ **27**, 2782 (2020). https://doi.org/10.1007/ s12540-020-00613-z.

[9]C. Lei and Y. Du, J. $Alloys\ Compd.$ **822**, 153674 (2020).

[10]N. Anzar, R. Hasan, M. Tyagi, N. Yadav, and J. Narang, $Sensor\ Int.$ **1**, 100003 (2020).

[11]L. Vovchenko, L. Matzui, V. Oliynyk, Y. Milovanov, Y. Mamunya, N. Volynets, A. Plyushch, and P. Kuzhir, $Materials$ **13**, 1118 (2020).

[12]B. Earp, J. Simpson, J. Phillips, D. Grbovic, S. Vidmar, J. McCarthy, and C. C. Luhrs, Nanomaterials. **9**, 491 (2019).

[13]A. Plyushch, D. Lyakhov, M. Simenas, D. Bychanok, J. Macutkevic, D. Michels, J. Banys, P. Lamberti, and P. Kuzhir, $Appl.Sci.$ **10**, 1315 (2020).

[14]H. Jia, Q. Q. Kong, Z. Liu,X. X. Wei,X. M. Li, J. P. Chen,F. Li,X. Yang, G. H. Sun, and C. M. Chen, $Compos.A\ Appl.Sci.$ **129**, 105712(2020).

[15]S. H. Park and J. H. Ha, $Materials$ **12**, 1395 (2019).

[16]Z. P. Wu, D. M. Cheng, W. J. Ma, J. W. Hu, Y. H. Yin, Y. Y. Hu, Y. S. Li, J. G. Yang, and Q. F. Xu, $AIP\ Adv.$ **5**, 067130 (2015).

[17]P. Gairola, L. P. Purohit, S. P. Gairola, P. Bhardway, K. Shivani, $Prog.Nat.Sci.$ **29**, 170 (2019).

[18]P. Raju, J. Shankar, J. Anjaiah, and S. R. Murthy, $AIP\ Conf.Proc$. 2162 (2019) 020027.

[19]S. Kumar, A. Ohlan, P. Kumar, and V. Verma, J. Supercond. $Nov.Magn.$ **33**, 1187 (2020).

[20]V. Tunakova, M. Tunak, V. Bajzik, L. Orechetna, S. Arabuli, O. Kyzymchuk, and V. Vlasenko, J. Eng. $Fiber\ Fabr$. 2020. doi:10.1177/1558925020925397.

[21]J. Kruželák, A. Kvasničáková, K. Hložeková, and I. Hudec, $Nanoscale\ Adv.$ **3**, 123 (2021).

[22]M. H. Al-Saleh, W. H. Saadeh, and U. Sundararaj, $Carbon$ **60**, 146 (2013).

[23]J. Kruželák, A. Kvasničáková, R. Plavec, E. Ušák, M. Ušáková, R. Dosoudil, and I. Hudec, $Polym.Adv.Technol.$ **31**,3272 (2020).

[24]A. Sarvi and U. Sundararaj, $Macromol.Mater.Eng.$ **299**, 1013 (2014).

[25]A. Prokopchuk, I. Zozulia, Y. Didenko, D. Tatarchuk, H. Heuer, and Y. Poplavko, $Coatings$ **11**, 172 (2021).

[26]G. Petrossian, N. Aliheidari, and A. Ameli, J. $Compos.Sci.$ **4**, 137 (2020).

[27]T. K. Gupta, B. P. Singh, V. N. Singh, S. Teotia, A. P. Singh, I. Elizabeth, S. R. Dhakate, S. K. Dhawan, and R. B. Mathur RB J. Mater. $Chem.A$ **2**, 4256 (2014).

[28]M. Marin-Genesca, J. Garda-Amoros, R. Mujal-Rosas, L. Massagues, and X. Colom, $Polymers$ **12**, 1075 (2020).

[29]R. Kumaran, M. Alagar, S. D. Kumar, V. Subramanian, and K. Dinakaran, $Appl.Phys.Lett.$ **107**, 113107 (2015).

[30]R. S. Yadav, I. Kuřitka, J. Vilcakova, M. Machovsky, D. Skoda, P. Urbánek, M. Masař, M. Jurča, M. Urbánek, L. Kalina, and J. Havlica, $ACS\ Omega.$ **4**, 22069 (2019).

[31]Z. W. Li and Z. H. Yang, J. Magn. $Magn.Mater.$ **391**, 172 (2015).

[32]J. Kruželák, A. Kvasničáková, E. Ušák, M. Ušáková, R. Dosoudil, and I., Hudec, $Polym.Adv.Technol.$ **31**, 1624 (2020).

[33]V. Shukla, $Nanoscale\ Adv.$ **1**, 1640 (2019).

[34]X. Wang, J. $Electromagn.Anal.Appl.$ **3**, 160 (2011).

[35]S. Sankaran, K. Deshmukh, M. Basheer Ahamed, S. K. Khadheer Pasha, $Compos.Part\ A$ **114**,49 (2018).

[36]B. Zhao, M. Hamidinejad, S. Wang, P. Bai, R. Che, R. Zhang, and C. B. Park, $J.Mater.Chem.A.$ **9**, 8896 (2021).

[37]Y. Bhattacharjee and S. Bose, $ACS\ Appl.Nano.Mater.$ **4**, 949 (2021).

[38]M. Derakhshani, E. Taheri-Nassaj, M. Jazirehpour, and S. M. Masoudpanah, $Sci.Rep.$ **11**, 9468 (2021).

[39]J. Prasad, A. K. Singh, M. Tomar, V. Gupta, and K. Singh, $Ceram.Int.$ **47**, 15648 (2021).

[40]S. Acharya and S. Datar, J. $Appl.Phys.$ **128**, 104902 (2020).